INTEGRATION OF A PRECOLOURING MATRIX IN THE RANDOM DEMODULATOR MODEL FOR IMPROVED COMPRESSIVE SPECTRUM ESTIMATION

D. Karampoulas, L. S. Dooley, S .M. Kouadri

Department of Computing and Communications, The Open University, Milton Keynes, UK.

ABSTRACT

The *random demodulator* (RD) is a *compressive sensing* (CS) architecture for acquiring frequency sparse, bandlimited signals. Such signals occur in cognitive radio networks for instance, where efficient sampling is a critical design requirement. A recent RD-based CS system has been shown to effectively acquire and recover frequency sparse, high-order modulated multiband signals which have been precoloured by an *autoregressive* (AR) filter. A shortcoming of this AR-RD architecture is that *precolouring* imposes additional computational cost on the signal transmission system. This paper introduces a novel CS architecture which seamlessly embeds a *precolouring matrix* (PM) into the signal recovery stage of the RD model (*i*PM-RD) with the PM depending only upon the AR filter coefficients, which are readily available. Experimental results using sparse wideband *quadrature phased shift keying* (QPSK) and 64 *quadrature amplitude modulation* (64QAM) signals confirm the *i*PM-RD model provides improved CS performance compared with the RD, while incurring no performance degradation compared with the original AR-RD architecture.

Index Terms— precolouring matrix, autoregressive filter, random demodulator, spectral leakage

1. INTRODUCTION

Compressive sensing (CS) is an efficient strategy for both signal acquisition and recovery at much lower sampling rates than the Nyquist theorem mandates [1, 2]. One of the key challenges which have given impetus to CS is the continually increasing requirements on traditional *analogue-to-digital converters* (ADC) which operate at the Nyquist sampling rate. Example application domains where such challenges arise include *cognitive radio* (CR) networks, where wideband signals, with high sampling rate requirements are encountered. A necessary constraint for efficient CS is that the signal must be sparse in some domain, i.e., Fourier, so it can be represented by a smaller number of significant frequency components than its bandwidth implies [3, 4]. This is often the case in wireless networks, where signals are intrinsically sparse in the frequency domain because of spectrum underutilization [5]. The greater the sparsity, the more efficient the signal acquisition and subsequent recovery [1-4].

The *random demodulator* (RD) is a CS architecture which is able to effectively acquire and recover signals which are bandlimited, periodic and sparse in nature [6]. It has been recently shown [7, 8] the RD can efficiently acquire and recover the *power spectral density* (PSD) of high-order modulated multiband signals, such as *quadrature phased shift keying* (QPSK), *binary* PSK (BPSK) 16 *quadrature amplitude modulation* (16QAM) and 64QAM. These modulation schemes are widely encountered in various wireless networking standards including: the IEEE 802.22 standard for CR [9], the IEEE 802.16 standard for *Worldwide Interoperability for Microwave Access* (WiMax) [10], and the 3rd Generation Partnership Project (3GPP) long term evolution (LTE) standard [11].

The reason for the improved RD performance with these signal types is that the input is firstly *precoloured* using an *autoregressive* (AR) filter to enhance signal sparsity. This amplifies the more significant spectral components, while concomitantly attenuating those lying outside the bands of interest. To select the best *precolouring* AR filter order, a nexus between filter order and CS performance for the AR-RD model has been established [7] to facilitate efficient PSD recovery.

A limitation of the AR-RD design is that the *precolouring* step is a separate pre-processing block to the RD. This is a consequence of not implementing a high-speed ADC within the AR filter, which offsets the benefit derived from using the innately lower sampling rates of the RD [7]. This however, imposes additional computational overheads on the transmission system, such as for example, licensed *primary users* (PU) in a CR network. Furthermore, the *precolouring* process affects the information content of the signal, since it alters the input sample values. This provided the motivation to investigate seamlessly integrating *precolouring* into the RD architecture to remove these inherent constraints.

This paper presents a novel RD architecture which seamlessly integrates a *precolouring matrix* (PM) into the signal recovery stage, which generates the PSD of the input signal. The new *i*PM-RD model crucially avoids the need for pre-processing of the RD input signal, with the only prerequisite being *a priori* knowledge of the AR filter coefficients, which form the individual PM elements. The benefit of this CS implementation in a CR context for example, is that it

no longer imposes burdens upon the PU, since currently mobile telecommunications providers already determine and transmit AR coefficients for speech coding purposes [12, 13], so the required PM elements will be available. Furthermore, the PM promotes greater sparsity in the RD so enhancing the signal recovery performance.

The experimental results corroborate that integrating the PM into the AR-RD structure provides improved spectral leakage performance compared with the original RD architecture [6], while no performance degradation is incurred in comparison with the scenario where *precolouring* is applied as a preprocessing block to the RD [8].

The remainder of the paper is organized as follows. Section 2 presents a brief overview of the AR-RD structure, while Section 3 details the role and construction of the PM within the AR-RD architecture. Experimental results are presented in Section 4, with some concluding comments being provided in Section 5.

2. AN OVERVIEW OF THE AR-RD STRUCTURE

The original AR-RD model [7,8] depicted in Fig. 1, consists of three constituent parts, with the AR filter *precolouring* the input signal $x(n)$, the RD subsampling the signal below the Nyquist rate and the recovery block estimating the signal PSD $S_c(f)$

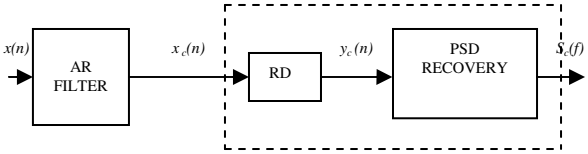

Fig. 1. The original AR-RD structure [7]

Precolouring is performed by an AR filter which has the generalised form [14, 15]:

$$x_c(n) = x(n) + \sum_{k=1}^{p} a_k x_c(n-k) \qquad (1)$$

where a_k are the filter coefficients optimally calculated using the modified covariance method [15] and p is the filter order, which is pragmatically chosen as $p=4$ in accordance with [8]. *Precolouring* $x(n)$ has the effect of either significantly reducing or eliminating the weaker frequencies lying outside the bands of interest, while sharpening the dominant spectral components, so increasing signal sparsity and ultimately the CS performance of the AR-RD structure.

The classic RD CS structure shown within the dotted lines in Figure 1, performs three functions [3, 6]; the input signal is firstly multiplied by a pseudorandom sequence which alternates at least at the Nyquist rate N, then it is low-pass filtered before it is captured at a sub-Nyquist rate $M<N$. If the *precoloured* signal $x_c(n)$ is employed as input, then the RD can be formalised as:

$$\boldsymbol{y_c} = A\boldsymbol{x_c} \qquad (2)$$

where $\boldsymbol{x_c}$ and $\boldsymbol{y_c}$ are the vector forms of $x_c(n)$ and $y(n)$ respectively, and A is an M x N measurement matrix. An example of A for $M=3$ and $N=9$ has the following form [3, 17]:

$$A = \begin{bmatrix} 1 & -1 & 1 & 0 & 0 & 0 & 0 & 0 & 0 \\ 0 & 0 & 0 & 1 & 1 & -1 & 0 & 0 & 0 \\ 0 & 0 & 0 & 0 & 0 & 0 & -1 & -1 & 1 \end{bmatrix} \qquad (3)$$

In general, A is a banded matrix with N/M non-zero consecutive entries at each row starting in column $rN/M+1$, with $r=0,1,...,M-1$ [3, 6].
If $\boldsymbol{f_c}$ is the Fourier representation of $\boldsymbol{x_c}$, then:

$$\boldsymbol{f_c} = F\boldsymbol{x_c} \quad \text{or} \quad \boldsymbol{x_c} = F^{-1}\boldsymbol{f_c} \qquad (4)$$

where F the N x N *discrete Fourier transform* (DFT) matrix. Using (4), (3) can now be expressed as:

$$\boldsymbol{y_c} = A\boldsymbol{x_c} = AF^{-1}\boldsymbol{f_c} = G\boldsymbol{f_c} \qquad (5)$$

where $G = A\,F^{-1}$. Signal recovery and subsequent calculation of $S_c(f)$ is accomplished by solving (5) for $\boldsymbol{f_c}$ using l_1*-norm minimization* [4, 18].

3. INTEGRATION OF PM INTO THE RD ARCHITECTURE

The *precolouring* AR process in Fig. 1 is performed prior to the input signal being sub-sampled by the RD and so is not an integral part of the CS framework. This levies a computational cost upon the signal transmission systems, as well as affecting the signal information content by altering signal sample values.

To resolve these overheads, this paper introduces the *i*PM-RD model which seamlessly embeds *precolouring* into the RD by formulating a PM at the signal PSD recovery stage, which solely depends on the AR coefficients, which are readily available as discussed in Section 1. The PM is derived from (3) and can be expressed as:

$$\boldsymbol{x}_c = C\boldsymbol{x} \qquad (6)$$

where $\boldsymbol{x}_c$ and $\boldsymbol{x}$ are the vector expressions of $x_c(n)$ and $x(n)$ respectively, while C is the PM of dimensions N x N. C is a lower triangular Toeplitz matrix with all main diagonal elements equal to one and the nonzero entries being functions of the a_k coefficients. Since the determinant of the PM is always one, C is guaranteed invertible, so from (3) and (6):

$$\boldsymbol{y_c} = A\boldsymbol{x_c} = AC\boldsymbol{x} = A_c\boldsymbol{x} \qquad (7)$$

where $A_c = AC$, which means that provided A_c is used as the measurement matrix, then the RD is able to perform *precolouring*. A_c is however, no longer a banded matrix and does

$$C = \begin{bmatrix} 1 & 0 & 0 & . & . & . & 0 \\ c_1 & 1 & 0 & . & . & . & 0 \\ c_2 & c_1 & 1 & . & . & . & 0 \\ . & c_2 & c_1 & . & . & . & 0 \\ . & . & . & . & . & . & . \\ c_{N-1} & . & . & . & . & 1 & 0 \\ c_N & c_{N-1} & . & . & c_2 & c_1 & 1 \end{bmatrix} \quad (8)$$

not have the same structure as A in (3). For this reason it cannot perform the functions of the RD, so instead C is integrated into the recovery stage of the model, so the RD now acts upon $\boldsymbol{x}$ instead of $\boldsymbol{x_c}$, as follows:

$$\boldsymbol{y} = A\boldsymbol{x} \quad (9)$$

From (4) and (6), it is implied that:

$$\boldsymbol{f_c} = F\boldsymbol{x_c} = FC\boldsymbol{x} \quad \text{or} \quad \boldsymbol{x} = C^{-1}F^{-1}\boldsymbol{f_c} \quad (10)$$

which is always valid because C is invertible. Thus, (8) can be expressed as:

$$\boldsymbol{y} = A\boldsymbol{x} = AC^{-1}F^{-1}\boldsymbol{f_c} = G_c\boldsymbol{f_c} \quad (11)$$

where $G_c = AC^{-1}F^{-1} = AF_c^{-1}$. The frequency vector $\boldsymbol{f_c}$ is derived by applying *l_1-norm minimization* to (10) and the PSD subsequently estimated from $\boldsymbol{f_c}$. This theoretical derivation shows that by using G_c instead of G, the PSD recovery stage can undertake *precolouring*, so the AR filter in Fig. 1 becomes obsolete, since all that is required is the set of α_κ coefficients to form C. G_c in (11) implies the sparsity basis matrix is now $F_c = FC$, which is tailored to the input signal by the PM coefficients. The corollary is this promotes greater sparsity in terms of basis representation. It is also apparent that for both *precolouring* approaches i.e., applied as an RD preprocessing block and applying the PM in the signal recovery stage, the same frequency vector $\boldsymbol{f_c}$ is obtained. A block diagram of the *i*PM-RD design is shown in Fig. 2, where *precolouring* in the PSD recovery stage of the RD is highlighted by the thick-lined boxes which relate to (7) and (11).

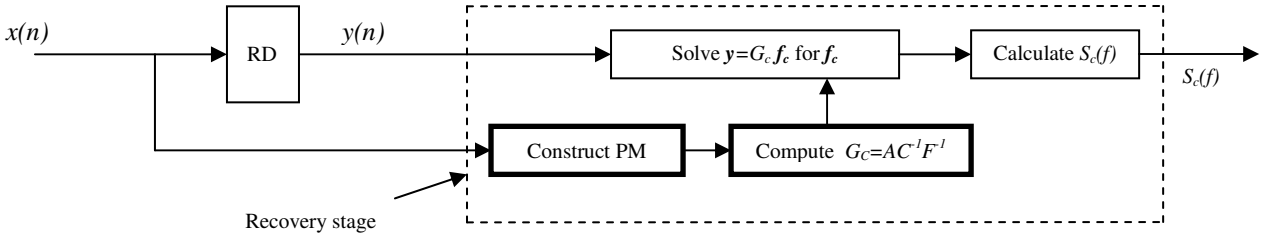

Fig.2. Block diagram of the *i*PM-RD architecture

4. SIMULATION RESULTS

The comparative performance of the *i*PM-RD model in Fig. 2 has been evaluated against the AR-RD (Fig. 1) and RD structures respectively. Experiments were undertaken upon a MATLAB-based platform using two QPSK/64QAM modulated test signals, with each being of 300ms duration and bit-rate of 215bps with two bands centered at carrier frequencies of 1kHz and 2.5kHz respectively. The sampling frequency was chosen 1.67 times greater than the Nyquist rate which corresponds to a signal length of 2048 samples.

The CS performance was analyzed at sub-sampled rates of 68%, 34%, 17%, 8.5% and 4.25% of the Nyquist rate which corresponds to 1024, 512, 256, 128 and 64 samples respectively. These test signals have been also employed in [7, 8] when the original AR-RD CS design was introduced. It is assumed that *x(n)* has additive white Gaussian (AWG) noise so the input *signal-to-noise ratio* (SNR) was set to 8.1dB and 15.6dB for QPSK and 64QAM respectively, as prescribed in the IEEE 802.22 standard for CR [19,20].

To critically evaluate the performance of the *i*PM-RD model the corresponding signal PSD was estimated and compared with both the classic RD and original AR-RD structure [7, 8], with *precolouring* applied directly to the input. The corresponding signal energies were then measured in the bands of interest at various sub-Nyquist sampling rates. The results for both QPSK and 64QAM modulation types are plotted in Fig. 4, where the total energy content percentage outside the bands of interest is termed the *PSD spectral leakage*.

The results for the *i*PM-RD model show the PM enhances sparsity with the average spectral leakage improving by ≈36% and ≈33% respectively for QPSK and 64QAM modulations compared with the basic RD. In addition, for both modulation types the spectral leakage is consistently lower than 20% for the PM case, even when the sampling rate falls below 5% of Nyquist, compared with more than 30% when *precolouring* is not applied.

To appraise the robustness of *i*PM-RD to input SNR, Fig. 5 displays the respective results for the two test modulation signals at various AWG noise levels. The sampling rate was arbitrarily chosen at 34% of the Nyquist rate,

though other sub-Nyquist rates are equally applicable. The results conclusively reveal that for both QPSK and 64QAM modulations the spectral leakage is lower than 20% across the entire input SNR range, when the PM is integrated into the RD structure, compared with more than 30% and 20% respectively for the original RD structure [6].

The influence of the greater sparsity which the PM promotes is illustrated in Fig. 6(a) and 6(b), which plots the recovered PSD for the RD and *i*PM-RD models respectively, for 64QAM at a sampling rate 4.25% of Nyquist. Despite being a very low sampling rate, the occupied bands are still able to be readily identified by *i*PM-RD, in contrast to the RD. Similar performance improvements can be observed for the QPSK test signals.

Finally, to validate the theoretical *i*PM-RD framework presented in Section 3, a comparative performance analysis with the original AR-RD model is given in Table 1 for QPSK modulation. This confirms the two CS architectures exhibit equivalent PSD spectral leakage performance and input SNR robustness, with a similar trend being evident for 64QAM.

5. CONCLUSION

This paper has presented an *integrated* PM-RD (*i*PM-RD) compressive spectrum (CS) estimation model for sparse, digitally modulated multiband signals, by embedding a *precolouring matrix* (PM) into the signal recovery stage. The PM is derived from the AR filter coefficients employed by signal providers for data compression purposes. Experimental results for higher-order digital modulation schemes such as QPSK and 64QAM, have compellingly shown the *i*PM-RD CS spectrum estimation structure consistently provides reduced PSD spectral leakage, while concomitantly being more robust to input SNR. Moreover, *i*PM-RD provides equivalent capability in terms of PSD spectral leakage reduction, compared with its original counterpart. Future research will investigate incorporating *precolouring* and the PM into other CS techniques, such as the compressive multiplexer, as well as formulating a computational complexity analysis for the *i*PM-RD model.

Sampling Rate (% Nyquist)	PSD Spectral leakage (%) *i*PM-RD	PSD Spectral leakage (%) original AR-RD
4.25	21.3	21.3
8	13.9	13.9
17	12.2	12.2
34	7.9	7.9
68	4.6	4.6

Table 1. PSD spectral leakage comparison at different sampling rates for the *i*PM-RD and AR-RD models for QPSK modulation

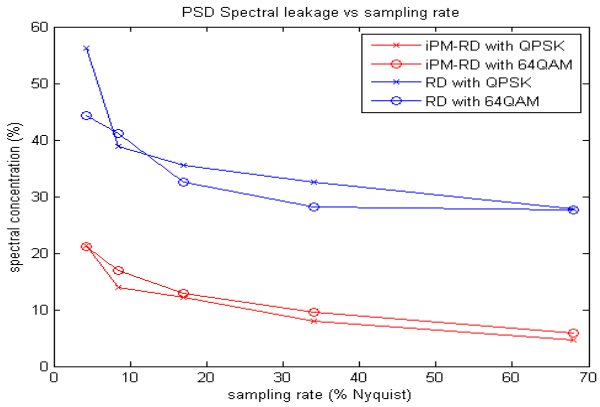

Fig. 4. PSD spectral leakage results showing the impact of using the PM for the QPSK and 64QAM test signals at various sampling rates

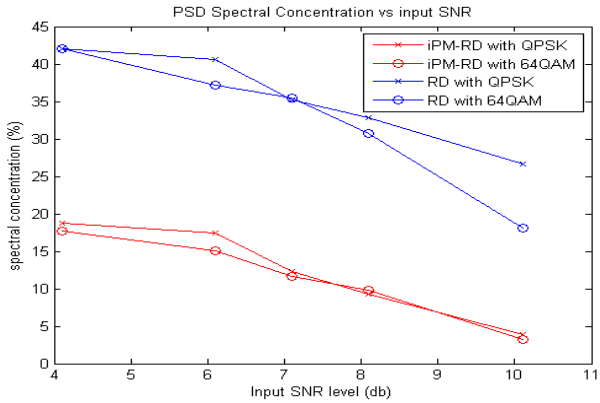

Fig. 5. Effect of the PM on the PSD spectral leakage results for the QPSK and 64QAM test signals for various SNR

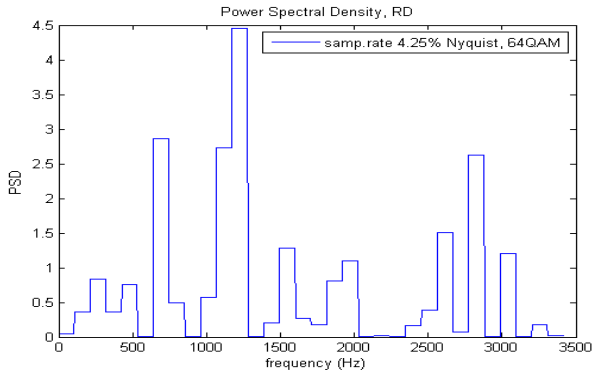

(a)

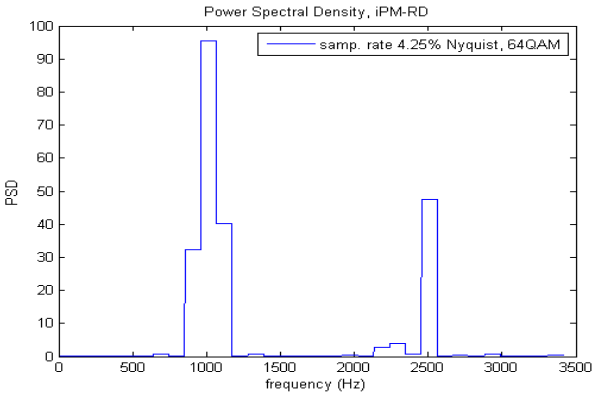

(b)

Fig. 6. Recovered normalised PSD (W/Hz) at a sampling rate of 4.25% Nyquist for: (a) RD and (b) *i*PM-RD

REFERENCES

[1] E. J. Candès, J. Romberg, T. Tao, "Robust uncertainty principles: Exact signal reconstruction from highly incomplete frequency information", IEEE Trans. Information Theory, vol. 52, no. 2, pp. 489-502, Feb. 2006.

[2] D. L. Donoho, "Compressed sensing", IEEE Transactions on Information Theory, vol. 52, pp. 1289-1306, Apr. 2006

[3] R. Baraniuk, M. A. Davenport, M. F. Duarte and C. Hegde, "An Introduction to Compressive Sensing". [Online]. Available: "http://cnx.org/content/col11133/1.5", (Accessed 5-06-2014).

[4] E. Candès, M. Wakin, "An Introduction To Compressive Sampling", IEEE Signal Processing Magazine, Vol.25, Issue 2, pp. 21-30, Mar. 2008.
.

[5] Federal Communications Commission, "Spectrum Policy Task Force" Rep. ET Docket no. 02-135, Nov. 2002.

[6] J. A. Tropp, J. N. Laska, M. F. Duarte, J. K. Romberg and R. G. Baraniuk, "Beyond Nyquist: Efficient sampling of sparse bandlimited signals'', IEEE Transactions On Information Theory, Vol. 56, No. 1, pp.520-544, Jan. 2010.

[7] D. Karampoulas, L.S. Dooley and S.K. Moustéfaoui, "Precolouring in Compressive spectrum estimation for cognitive radio", IEEE EUROCON, pp. 1715-1720, Zagreb, Jul. 2013.

[8] D. Karampoulas, S. M. Kouadri and L.S. Dooley, "A novel precolouring-random demodulator architecture for compressive spectrum estimation", IET/ISP Conference, pp.1-6, London, Dec. 2013.

[9] A. N. Mody, G.Chouinard, "IEEE 802.22 Wireless regional area networks", IEEE 802.22-10/0073r03, Jun. 2010.

[10] J. Rakesh, W. Vishal, U. Dalal, "A survey of mobile WiMax IEEE 802.16m standard", International Journal of Computer and Information Security, vol.8, no. 1, pp.125-131, Apr. 2010.

[11] 3GPP TR 36.814 V9.0.0 (technical report), Mar. 2010.

[12] J. Proakis, *"Wiley Encyclopedia of Communications"*, Vol. 5, N. Jersey, USA, Wiley-Interscience.

[13] L. Deng, D. O'Shaughnessy, "*Speech Processing: A dynamic and optimization-oriented approach (Signal Processing and Communications)*, CRC Press, New York, 2003.

[14] D. Manolakis, V. Ingle, S. Kogon, "*Statistical and Adaptive Signal Processing*", Artech House, Boston, USA, 2005.

[15] S.L. Marple, "*Digital Spectral Analysis with Applications*", Englewood Cliffs, New Jersey, USA, Prentice-Hall, 1987.

[16] R.Gitlin, J.Hayes and S.Weinstein, "*Data Communications*", Plenum Press, NewYork, 1992.

[17] T. Ragheb, J. N. Laska, H. Nejati, S. Kirolos, R. G. Baraniuk, and Y. Massoud "A prototype hardware for random demodulation based compressive Analog-to-Digital Conversion", 51st IEEE Midwest Symposium in Circuits and Systems, pp. 37-40, Aug. 2008.

[18] l1 Magic, a collection of MATLAB routines for solving the convex optimization programs central to compressive sampling. [Online]. Available: "http://www.l1-magic.org/", (Accessed 24-06-2013).

[19] M. Nekovee, "A survey of cognitive radio access to TV white spaces", Hindawi Publishing Corporation, International Journal of Digital Media Broadcasting, Vol. 2010, Article ID 236568, Apr. 2010.

[20] A. N. Mody, G.Chouinard, "IEEE 802.22 Wireless regional area networks", IEEE 802.22-10/0073r03, Jun. 2010.